Molecular Crystals and Liquid Crystals Science and Technology. Section A. Molecular Crystals and Liquid Crystals
Publication details, including instructions for authors and subscription information:
http://www.tandfonline.com/loi/gmcl19

Dynamical Response of Cholesteric Liquid Crystals Under Electric Fields

N. Scaramuzza [a b], V. Carbone [a b], C. Ferrero [a c] & C. Versace [a b]
[a] Dipartimento di Fisica, Universita della Calabria, 87036, Rende, (CS), ITALY
[b] Consorzio I.N.F.M., Unitàdi Cosenza
[c] European Synchrotron Radiation Facility, BP 200, F-38043, Grenoble, CEDEX, France
Version of record first published: 23 Sep 2006.

To cite this article: N. Scaramuzza , V. Carbone , C. Ferrero & C. Versace (1995): Dynamical Response of Cholesteric Liquid Crystals Under Electric Fields, Molecular Crystals and Liquid Crystals Science and Technology. Section A. Molecular Crystals and Liquid Crystals, 262:1, 379-390

To link to this article: http://dx.doi.org/10.1080/10587259508033541

Mol. Cryst. Liq. Cryst. 1995, Vol. 262, pp. 379–390
Reprints available directly from the publisher
Photocopying permitted by license only

DYNAMICAL RESPONSE OF CHOLESTERIC LIQUID CRYSTALS UNDER ELECTRIC FIELDS

N. SCARAMUZZA*, V. CARBONE*, C. FERRERO+ and C. VERSACE*
Dipartimento di Fisica , Universita' della Calabria, 87036 Rende (CS) ITALY
*) Consorzio I.N.F.M.; Unità di Cosenza.
+) Present address: European Synchrotron Radiation Facility, BP 200, F-38043 Grenoble CEDEX, France

Abstract: In a previous paper [1] we suggested that, in a cholesteric liquid crystal undergoing a step-like d.c. electric field applied parallel to the helical axis, the behavior of the relative variation of the maximum intensity wavelength of the Bragg-reflected light is related to two different relaxation phenomena. In this paper we present the time behavior of the relative variation of the maximum intensity wavelength of the Bragg-reflected light for different sample thicknesses. Moreover, the disagreement between the experimental behavior of relaxation times vs E and theoretical one ($\tau \sim 1/E^2$) can be related to an increase of the medium apparent viscosity which is due to the increase of dislocation density with the external applied field.

INTRODUCTION

Since many years it has been recognized that the orientation pattern of liquid crystals can be changed by magnetic and electric field. This phenomenon arise because of the diamagnetic, dielectric and conductivity anisotropy of liquid crystals.

Let us consider, for instance, a cholesteric liquid crystal (CLC) with positive dielectric anisotropy [$\Delta\epsilon = (\epsilon_{\parallel} - \epsilon_{\perp}) > 0$] and a planar orientation between two glass plates. If an

external electric field is applied perpendicularly to the walls of the cell, the experimentally observed deformation consist in a two-dimensional spatially periodic deformation which has the form of a square grid [1,2,3].

On the contrary, in the case of negative dielectric anisotropy, for the above mentioned reasons, we should expect the texture would be stabilized. Nevertheless, it has been found that also in this case instabilities can be generated by an external electric field in a reversible way. Infact, as there is positive anisotropy in the electrical conductivity [$\Delta\sigma = (\sigma_{\parallel} - \sigma_{\perp}) > 0$], a planar texture of cholesteric liquid crystal in an electric field perpendicular to the walls of the cell is unstable for any sign of $\Delta\epsilon$. The instability is due by the competition between the torque induced by the electrical conductivity acting and the elastic torque of the cholesteric, which also results in the appearance of a two-dimensional periodic pattern for the distribution of the director [4,5].

In a previous paper [6] we presented the study of the static deformations generated by a d.c. electric field in a CLC with $P_0/d \ll 1$ (where P_0 is the unperturbed pitch of the CLC and d is the sample thickness). Furthermore, we studied the optical properties [7] of a CLC sample in the same configuration with a particular regard to the rotatory power and the spectrum of reflected and transmitted light.

Using the technique reported in ref. [8], which allows us to study the time-resolved reflection spectrum of a CLC submitted to an external field, we studied the time-dependent behavior of a CLC undergoing mechanical deformations [9-12].

In the present paper, by means of the above mentioned technique, we study the dynamical behavior of the apparent pitch in a planar sample of a CLC, with positive dielectric anisotropy, subject to a step-like d.c. electric field applied parallel to the helical axis, for different sample thicknesses.

EXPERIMENTAL SET-UP AND RESULTS

Our observations has been performed on a cholesteric sample that is a room temperature mixture of cholesterol nonanoate, chloride and oleyl carbonate, with an equilibrium pitch P_0=0.4 μm, in a planar configuration. The dielectric anisotropy of this CLC was found to be positive [7], $\Delta\epsilon \cong 1$.

To prevent electrode effects and to obtain the planar texture, the indium oxide coating

the glass plates was covered by few tens Å thick SiO layer evaporated at an angle of 60° [13]. The sample width was L=1 cm and the sample thicknesses were determined by Mylar spacers.

The sample was illuminated by a white-parallel-light source at an angle of incidence of 30°. The Bragg-reflected light was analyzed by a monochromator followed by a BM Spektronix 512 diode-array system (AK 500), to perform time-resolved optical spectroscopy. For each fixed delay (10 ms -> ∞), we obtained a spectrum of the Bragg-reflected light, characterized by its maximum intensity wavelength P. The synchronization between the sample excitation and the data acquisition was achieved by a PC (Fig. 1).

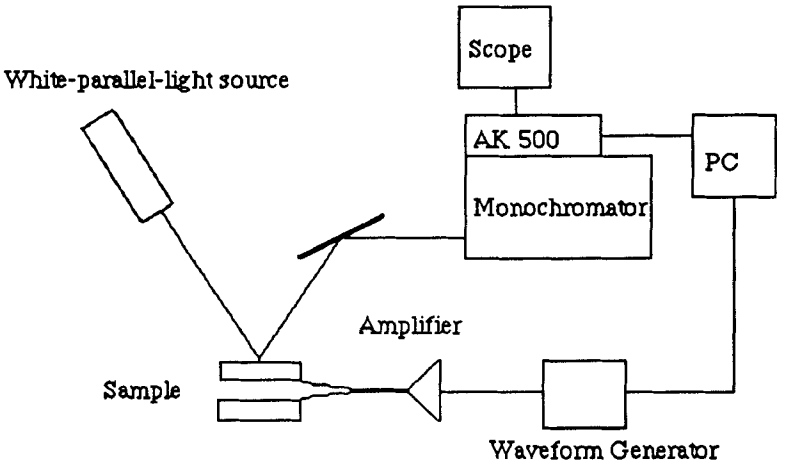

FIGURE 1. Experimental set-up. The diode-array are scanned by an electronic multiplexer and the reading was addressed in 8 ms to a buffer memory whose width amounted to 24 spectra. In the actual experimental set-up the detectable spectral width is 250 Å, which is more or less equal to the width of the Bragg reflection of the CLC sample. The synchronization between the sample excitation and the data acquisition was achieved by a PC.

We got the electric field parallel to the helical axis [z-axis] by applying a step-like voltage to the conductive glasses walls. The excitation frequency was low enough (10^{-3} Hz) to ensure that the external electric field was applied during all experimental measurements. The voltage was provided by an amplifier driven by a waveform generator.

In Fig. 2 are shown the instantaneous relative variation of the maximum intensity wavelength of the Bragg-reflected light [$\Delta P(t) = P(t) - P_0$] for two different thicknesses of the CLC sample. The quantity $\Delta P(t)$ diminishes in time in a manner that suggests us a behavior of the type:

$$\Delta P(E,t) = A(E)\, e^{-\frac{t}{\tau_L(E)}} + B(E)\, e^{-\frac{t}{\tau_S(E)}} + C(E) \qquad (1)$$

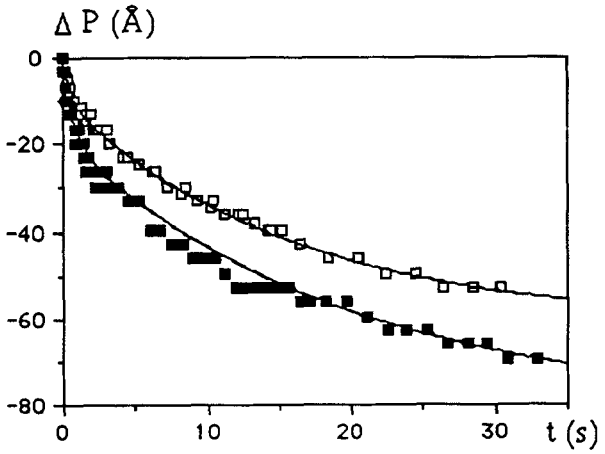

FIGURE 2. Instantaneous relative variation of the maximum intensity wavelength of the Bragg-reflected light [$\Delta P(t) = P(t) - P_0$]. White squares refer to the sample thickness of 50 μm and an applied electric field of 13 kV/cm. Black squares refer to the sample thickness of 100 μm and an applied electric field of 21 kV/cm. The solid lines represent the fits made by eq. (1).

Fitting eq. (1) on the experimental data by a least square method, we obtain, for each value of E, the characteristic times and the pre-exponentials.
In Fig.s (3 - 6) we show the behavior of $\tau_S(E)$ and $\tau_L(E)$ vs. E.

DISCUSSION

For the geometry under discussion here the experimentally observed deformation [14,15] is a two-dimensional spatially periodic deformation which has the form of a square grid,

with the size:

$$w = \left(\frac{3}{32}\frac{K_3}{K_2}\right)^{1/4}(P_0 d)^{1/2} \qquad (2)$$

The dielectric torque tends to re-orientate the molecules into an arrangement corresponding to the fingerprint texture. Instead, the elastic torque tends to preserve the cholesteric layers. If the applied electric field is equal or slightly above a threshold value for the deformation E_{th}, i.e. $E \approx E_{th}$, a pattern which undulates in x and y direction appears as a compromise alternative for the distribution of the director. The wave vector of this deformation pattern along the z-axis is approximately π/d [2].

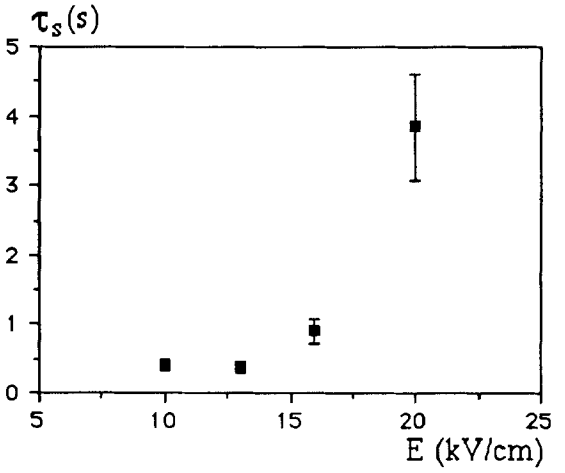

FIGURE 3. The faster characteristic times τ_S vs external applied field for the sample of thickness 50 μm.

When the intensity of the applied electric field is increased, the deviation angle of the director **n** also increases and it tends towards the limit $\theta=\pi/2$ in the whole volume [17].

In our experiment we apply to the CLC samples, step-like d.c. external electric fields which amplitude are greater than threshold ones. Infact, the obtained experimental threshold fields for the CLC material under investigation were found to be 3.60 kV/cm and 2.55 kV/cm for the 50 μm and 100 μm sample thickness respectively [7]. For this reason we think that, at first the CLC responds to external electric fields by the

establishment of the two dimensional spatially periodic deformation, followed, in time, by an increase of the angle of deviation of the director corresponding to a decrease of the period deformation size.

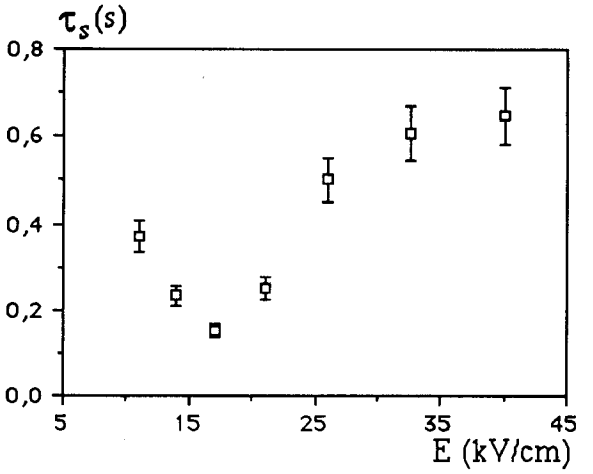

FIGURE 4. The faster characteristic times τ_S vs external applied field for the sample of thickness 100 μm.

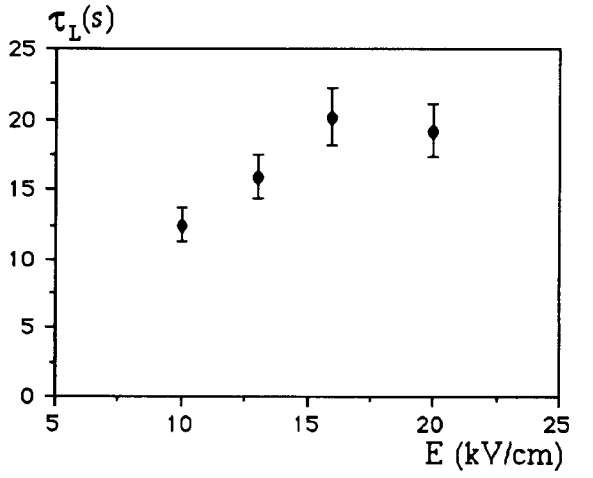

FIGURE 5. The slower characteristic times τ_L vs external applied field for the sample of thickness 50 μm.

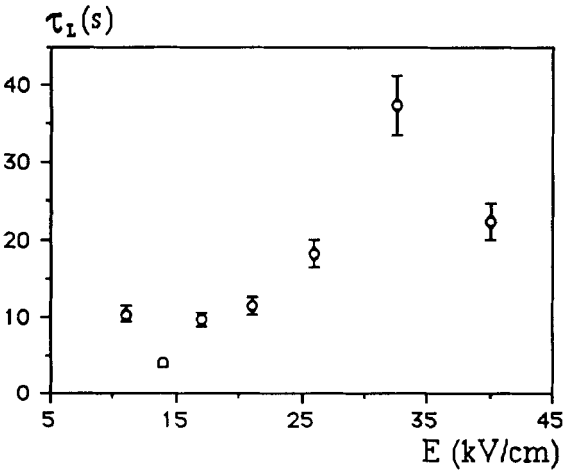

FIGURE 6. The slower characteristic times τ_L vs external applied field for the sample of thickness 100 μm.

Moreover, when the external electric field is further increased a large number of dislocations, which constitute an obstacle to the relaxation of the cholesteric structure, merges in the sample [18]. Since the number of dislocations increases with E until a certain value for which the increasing dielectric torque causes a breaking of the dislocations, we aspect that the medium apparent viscosity $\gamma_{app}(E)$ will increases with E up to a saturation value.

Under the small θ approximation, the equation of motion of the deviation angle θ of the director **n** may be obtained from the free energy function [3,17]

$$f = \frac{3}{16} K_3 (\frac{\pi}{w})^2 \theta^2 + \frac{1}{2} K_2 (\frac{q_0 w}{d})^2 - \frac{\Delta\epsilon}{8\pi} E^2 \theta^2 \qquad (3)$$

and from the dissipation function

$$D = \frac{1}{2} \gamma_{app}(E) (\frac{\partial\theta}{\partial t})^2 \qquad (4)$$

Then, the characteristic time for the establishment of the two-dimensional spatially periodic deformation is given by

$$\tau_S = \frac{\gamma_{app}(E)}{\frac{\Delta\epsilon}{4\pi} E^2 - [K_2(\frac{q_0 w}{d})^2 + \frac{3}{8} K_3(\frac{\pi}{w})^2]} \qquad (5)$$

As second step the angle θ continues to increase. This should excite wavevectors greater than $(w)^{-1}$, thus generating smaller spatial structures. The observed relaxation time is then related to the growth rate of a given wavevector q(E), and can be written in a way analogous to eq. (5) [1]

$$\tau_L = \frac{\gamma_{app}(E)}{\frac{\Delta\epsilon}{4\pi} E^2 - K[q(E)]^2} \qquad (6)$$

where K is an elastic constant.

Let us remember that the angle θ is related to the pitch variation ΔP [19], so that we can compare the experimentally obtained relaxation times with those derived from the theory.

From eq. (5) we found the discrete value of $\gamma_{app}(E)$, which are shown in Fig. (7) by black squares and white squares for the sample thickness of 50 μm and 100 μm respectively.

These experimental behaviors of $\gamma_{app}(E)$ suggests us the following heuristic function

$$\gamma_{app}(E) = \gamma_1 F(d) [1 + \tanh (\frac{E}{\tilde{E}(d)} - h(d)] \qquad (7)$$

which is represented in Fig. (7), taking $\gamma_1 = 1$, both for 50 μm and 100 μm thicknesses.

The values of the constants F, $\tilde{E}$ and h which have been determined by the fit are the following:

d = 100 μm F = 719.1 $\tilde{E}$ = 35.0 h = 3.1

d = 50 μm F = 655.7 $\tilde{E}$ = 8.1 h = 7.6 cgs units.

From Fig. (7) we can note that for a fixed value of external applied field, the medium apparent viscosity is greater for the thinner samples. This result could indicate that, at a

fixed value of applied electric field, the dislocation density is greater for thinner samples (obviously, supposing that the number of dislocation merging in the sample depend only on applied electric field, the dislocation density is greater in thinner samples).

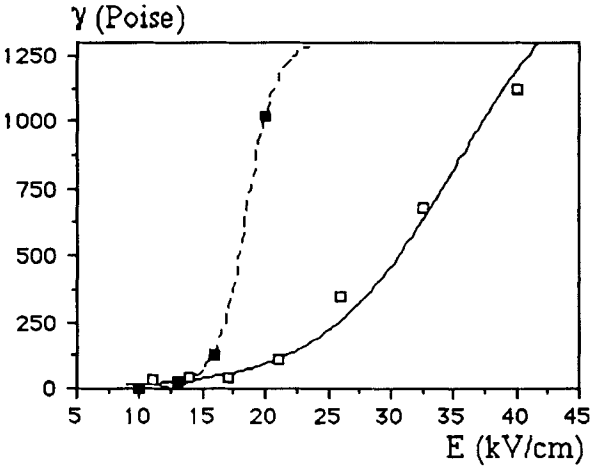

FIGURE 7. Behavior of $\gamma_{app}(E)$, cgs units, vs external applied electric field. Black squares and white squares refer to the 50 μm and 100 μm samples respectively. The values are calculated from the eq. (5) using the parameter values previously estimated by us for the examining material. The solid line represent the best fit made by eq. (7) for the sample thickness of 100 μm. The dashed line represent the best fit made by eq. (7) for the sample thickness of 50 μm.

By introducing the discrete values of $\gamma_{app}(E)$ into eq. (6), we found the corresponding values of q(E).

The sizes of the corresponding spatial structures $\Lambda(E) \approx \pi/q(E)$ are reported in Fig. (8) both for the 50 μm and the 100 μm samples respectively.

In order to confirm this result, we underline that, when the applied electric field tends to the threshold value E_{th}, $\Lambda(E)$ tends to the threshold value of the size of the two-dimensional spatially periodic deformation ($6 \cdot 10^{-4}$ and $4 \cdot 10^{-4}$ cgs units for the sample thickness of 50 μm and 100 μm respectively). Moreover, as long as the external electric field increases, $\Lambda(E)$ seems to tend to the value of the unperturbed pitch P_0. Obviously as $E \rightarrow \infty$ we expect a cholesteric-nematic transition.

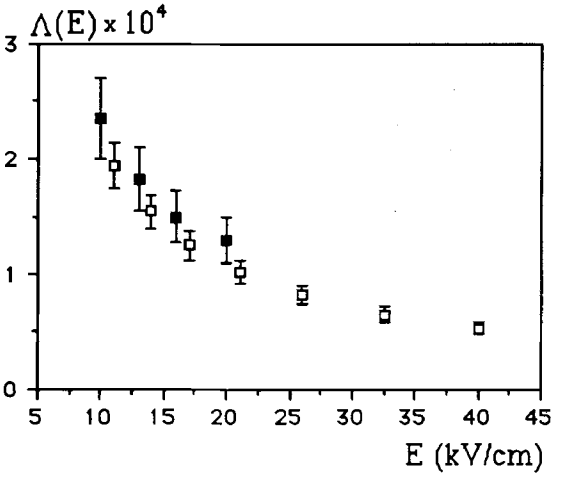

FIGURE 8. Behavior of Λ(E), cgs units, vs external applied electric field. Black squares and white squares refer to the sample thickness of 50 μm and 100 μm respectively.

CONCLUSION

In this paper we presented the time behavior of the relative variation of the maximum intensity wavelength of the Bragg-reflected light for different sample thicknesses. We have shown that the behavior of the relative variation of the maximum intensity wavelength of the Bragg-reflected light of a cholesteric liquid crystal, undergoing a step-like d.c. electric field applied parallel to the helical axis, is related to two different relaxation phenomena.

Moreover, the disagreement between the experimental behavior of relaxation times vs E and theoretical one ($\tau \sim 1/E^2$) can be related to an increase of the medium apparent viscosity which is due to the increase of dislocation density with external applied field.

Acknowledgement

The authors are greatly indebted with A. Alexe-Ionescu, G. Barbero , R. Bartolino and S.

A. Pikin for useful discussions and suggestions.

References

1. N. Scaramuzza, C. Ferrero, V. Carbone, C. Versace: submitted to *J. of Applied Phys.*
2. C.S. Gerritsma, P.van Zanten: *Phys. Lett.*; **37A**, 47 (1971).
3. F. Rondelez, H. Arnould, C. Gerritsma: *Phys. Rev. Lett.*; **28**, 735 (1972).
4. W.J.A. Goossens: *Phys. Lett.*; **40A**, 95 (1972)
5. I.W. Smith, Y. Galerne, S.T. Lagerwall, E. Dubois-Violette, G. Durand: *J. Phys. (Paris)*; **36**, C1-237 (1975)
6. F. Simoni, R. Bartolino, N. Scaramuzza: *Springer Verlag Series on Chem. - Phys.*; **11**, 205 (1980).
7. R. Bartolino, F. Simoni: *Optica Acta*; **27**, 1179 (1980).
   R. Bartolino, A. Ruffolo, F. Simoni, N. Scaramuzza: *Nuovo Cimento*; **1D**, 607 (1982).
8. N. Scaramuzza, N. Guarracino, F.P. Nicoletta, F. Simoni, R. Bartolino: *Applied Optics*; **25**, 1571 (1986).
9. N. Scaramuzza, V. Carbone, R. Barberi: *Mol. Cryst. Liq. Cryst.*; **195**, 31 (1991).
10. N. Scaramuzza, V. Carbone, J. P. Marcerou, R. Bartolino: *J. Appl. Phys.*; **67**, 169 (1990).
11. N. Scaramuzza, F. Simoni, R. Bartolino, G. Durand: *Phys. Rev. Lett.*; **53**, 2246 (1984).
12. V. Carbone, N. Scaramuzza, N. Guarracino: *Mol. Cryst. Liq. Cryst.*; **188**, 57 (1990).
13. M. Monkade, M. Boix, G. Durand, *Europhys. Lett.*; **5**, 697 (1988).
14. W. Helfrich, *Appl. Phys. Lett.*; **17**, 531, (1970).
15. J. P. Hurault, *J. Chem. Phys.*; **59**, 2068 (1973).
16. W. Helfrich: *J. Chem. Phys.*; **55**, 839 (1971).
17. L. M. Blinov: *Electro-Optical and Magneto-Optical Properties of Liquid Crystals*;

(Wiley-Interscience Publication, Belfast) 1983.

18. W. Helfrich: *Mol. Cryst. Liq. Cryst.*; **22**, 187 (1973).
19. N. Scaramuzza, R. Barberi, F. Simoni, F. Xu, G. Barbero, R. Bartolino: *Phys. Rev. A*; **32**, 1134 (1985).